Microscopic evidence of the connection between liquid-liquid transition and dynamical crossover in an ultraviscous metallic glass former

S. Hechler,[1,2] B. Ruta,[2,3,*] M. Stolpe,[1] E. Pineda,[4] Z. Evenson,[5] O. Gross,[1] A. Bernasconi,[2,6] R. Busch,[1] and I. Gallino[1]

[1]*Chair of Metallic Materials, Department of Materials Science and Engineering, Saarland University, Campus C6.3, 66123 Saarbrücken, Germany*

[2]*ESRF—The European Synchrotron, CS40220, 38043 Grenoble, France*

[3]*Univ Lyon, Université Claude Bernard Lyon 1, CNRS, Institut Lumière Matière, Villeurbanne, France*

[4]*Departament de Física, Universitat Politècnica de Catalunya–BarcelonaTech, ESAB, Esteve Terradas 8, 08860 Castelldefels, Spain*

[5]*Heinz Maier-Leibnitz Zentrum (MLZ) and Physik Department, Technische Universität München, Lichtenbergstrasse 1, 85748 Garching, Germany*

[6]*Dipartimento di Chimica, Università di Pavia, Viale Taramelli 16, 27100 Pavia, Italy*

(Received 14 September 2017; published 23 August 2018)

Liquid-liquid transitions are interesting to many researchers since they occur in systems as diverse as monoatomic liquids, multicomponent oxides, and metallic glass formers. In some cases, the crossover is accompanied by changes in the dynamical properties. By combining state-of-the-art synchrotron techniques, we followed the structure and atomic motion during quasistatic cooling of the $Au_{49}Cu_{26.9}Si_{16.3}Ag_{5.5}Pd_{2.3}$ metallic glass former from the low-temperature supercooled liquid. With this thermal protocol, we were able to lower the glass transition temperature far enough to reveal a liquid-liquid crossover between two amorphous structures corresponding to two ultraviscous liquids with different kinetic behavior. This transition is in competition with vitrification, which occurs at conventional cooling rates, and is accompanied by structural changes not affecting the average density. Our results provide a direct connection between polyamorphism and dynamical crossover, and an alternative case to add to the highly debated topic on the low-temperature divergence of the dynamics in supercooled liquids.

DOI: 10.1103/PhysRevMaterials.2.085603

I. INTRODUCTION

Many systems, ranging from monoatomic liquids [1–3] to amorphous alloys [4–7], exhibit transitions between liquid phases of different structure. In glass formers, liquid-liquid transitions (LLTs) have been reported either in high-temperature melts [3,8–13] or in supercooled liquids [4–6,14–17], suggesting the existence of intrinsic connections between the kinetic properties of the system and the transition temperature [18]. LLTs are sometime associated to a dynamical crossover with changes in the kinetic fragility [6,10,16,19]. When observed upon cooling, the liquid evolves from a high-temperature fragile phase with a steep temperature dependence of viscosity and structural relaxation time, to a strong phase less affected by temperature changes. By combining macroscopic calorimetric measurements and phase contrast imaging, Kurita and Tanaka showed that the fragility of a molecular liquid can be tuned by the same parameters controlling the LLT [16]. For fragile liquids, the LLT is, however, expected at such a low temperature that the system may arrest beforehand in the glass [18].

By taking advantage of state-of-the-art synchrotron techniques like x-ray photon correlation spectroscopy (XPCS) and high-energy x-ray diffraction (XRD), we present experimental measurements of the microscopic dynamics of an ultraviscous glass former with long relaxation times which were not accessible until now, neither experimentally nor with numerical simulations. We find the occurrence of a LLT upon quasistatic cooling of the $Au_{49}Cu_{26.9}Si_{16.3}Ag_{5.5}Pd_{2.3}$ metallic glass former, which can be *directly connected* with a fragile-to-strong dynamical crossover. Our thermal approach consists of isothermal steps of 0.5 K at a cooling rate of 0.1 K min^{-1} in the supercooled region between 396 and 380 K (see the Supplemental Material [20] for more details on the thermal protocol). With this protocol the glass transition temperature, T_g, is lowered more than 30° in comparison to a standard cooling rate of 20 K min^{-1}, allowing us to unveil the polyamorphic crossover in the ultraviscous regime, predicted also by Ref. [18]. Interestingly, while the kinetic transition seems to occur at a determined temperature and leads to stationary dynamics, the structure exhibits much slower transformation rates over a broader transition region. This scenario provides a unique picture of polyamorphism at the atomic level and supports the idea of the formation of an alternative liquid phase that is locally more ordered and which does not affect the average density, as suggested in different complex systems [16,21–25].

II. RESULTS

A. Dynamical data

XPCS experiments were performed at beamline ID10 at ESRF, France. Technical details are reported in the Supplemental Material [20]. Figure 1 shows a selection of data measured at

*beatrice.ruta@univ-lyon1.fr

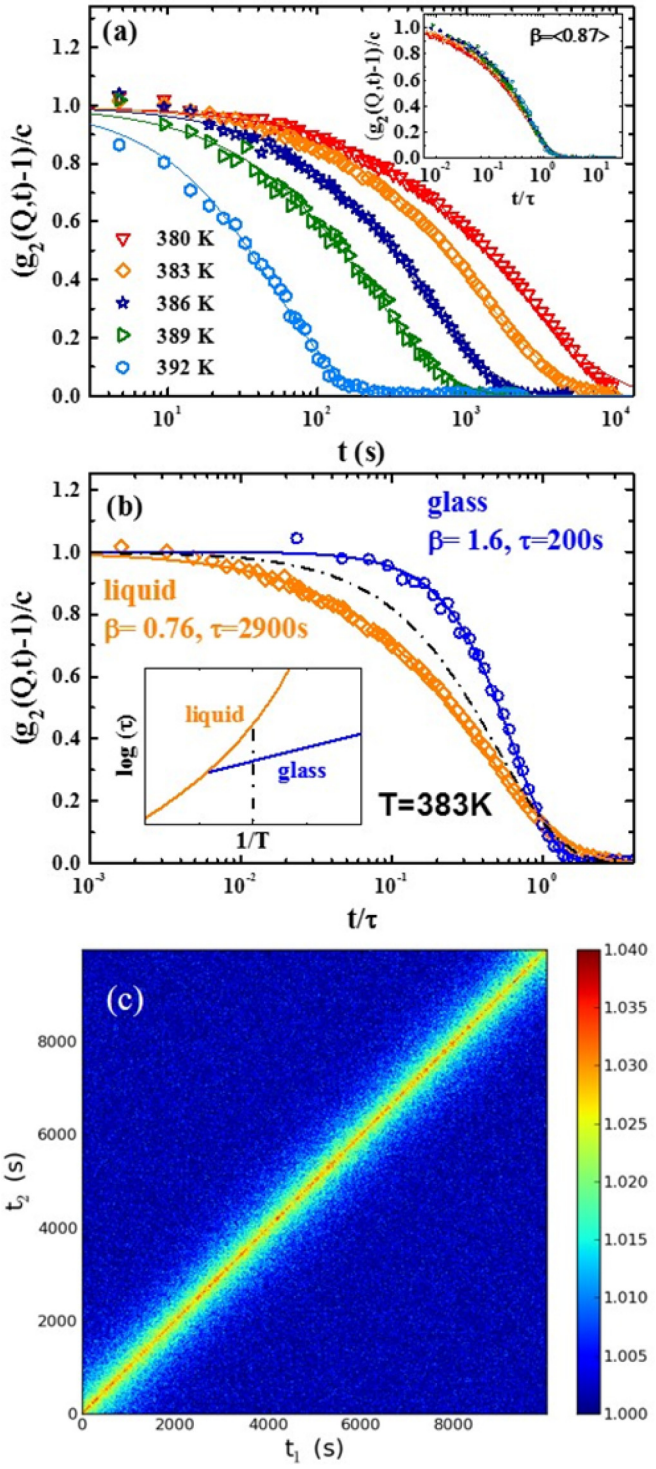

FIG. 1. (a) Temperature dependence of normalized intensity autocorrelation functions measured with XPCS at $Q_p = 2.78\,\text{Å}^{-1}$. Lines are fits using the KWW function. Inset: Same data reported as t/τ. (b) $g_2(Q_p, t)$–1/c as a function of t/τ measured at 383 K in a hyperquenched glass heated from low temperature (blue circles), and in the supercooled liquid shown in panel (a) (orange diamonds). The dashed line is a single exponential decay. The two curves correspond to two distinct dynamics as sketched in the inset by the intersection of the vertical line with the glass or the liquid. (c) TTCF at 386 K showing stationary dynamics.

a wave vector $Q_p = 2.78\,\text{Å}^{-1}$ corresponding to the maximum of the structure factor, $S(Q)$, for different isothermal steps between 392 and 380 K during cooling from the liquid. These temperatures lie slightly above the T_g for the applied cooling rate, which is 380 K, thus 33 K below the standard calorimetric $T_g^{\text{end}} = 413\,\text{K}$ (see Ref. [26] and the Supplemental Material [20] for more details on the cooling rate dependence of T_g). The time average intensity autocorrelation functions are reported in Fig. 1(a) together with the fits with a Kohlrausch-Williams-Watts (KWW) function: $g_2(Q,t) = 1 + c\{\exp[-2(t/\tau)^{\beta}]\}$. Here, τ is the structural relaxation time, β the shape parameter, and c the product between the experimental contrast and the nonergodicity level of the glass, which is basically unity at Q_p [27]. All data are normalized by c, which is found constant at 4%. The $g_2(Q,t)$ are connected to the decay of density fluctuations and provide information on the collective dynamics at the probed length scale and time interval [28].

The behavior of supercooled liquid dynamics is seen in Fig. 1(a). (1) Longer time decays are observed upon cooling, with a dramatic shift of two orders of magnitude from $\sim 10^2$ to $\sim 10^4$ s in just 12 K. (2) The shape of the curve is described by a stretched parameter ($\beta < 1$) with average value of 0.87 ± 0.10, signature of the heterogeneous dynamics usually found in metallic glass formers [29–31]. (3) All data collapse onto a single curve when rescaled in reduced time units t/τ confirming the validity of time-temperature superposition [inset, Fig. 1(a)] [32–34].

The stretched shape of the $g_2(Q_p, t)$ in the supercooled liquid contrasts dramatically with the behavior observed in glasses. At the atomic level, metallic glasses exhibit stress-dominated dynamics characterized by an anomalous compressed decay of the correlation functions ($\beta > 1$) [30,35–38], reminiscent of that reported in some soft glasses [28,29] and related to microscopic elastic frustrations [39–41]. This is also the case for the system studied in this work. As an example, Fig. 1(b) shows two normalized $g_2(Q_p, t)$ rescaled as t/τ, both measured at 383 K but in two different amorphous states reached by following different thermal paths. Open diamonds correspond to a supercooled liquid obtained by applying the quasistatic cooling, while open circles are measured directly at 383 K in a glass produced by melt spinning (i.e., cooled with $\sim 10^6$ K/s). In the glass, the data decay fast and can be modeled with a compressed β *two times larger* than the value found in the liquid. Similar stretched $g_2(Q_p, t)$ for the liquid and compressed $g_2(Q_p, t)$ for the glass have been reported also in a Mg-based metallic glass former [36,42]. Remarkably, even if the data in Fig. 1(b) are measured at the same temperature, they correspond to dynamics that differ by a factor of 15 in time, as schematically shown in the inset, with $\tau_{\text{glass}} \sim 200$ s and $\tau_{\text{liquid}} \sim 3000$ s.

In the supercooled liquid, the system displays equilibrium dynamics. Figure 1(c) shows representative data at 386 K through the evolution of the two-times correlation function (TTCF), which describes the instantaneous correlation between intensity fluctuations in subsequent speckle patterns [28] (see the additional information on the XPCS measurements reported in the Supplemental Material [20]). The width of the intensity along the main diagonal is proportional to τ. The atomic dynamics appears stationary over the entire observation time of 9000 s, thus for a temporal interval ≈8 times larger

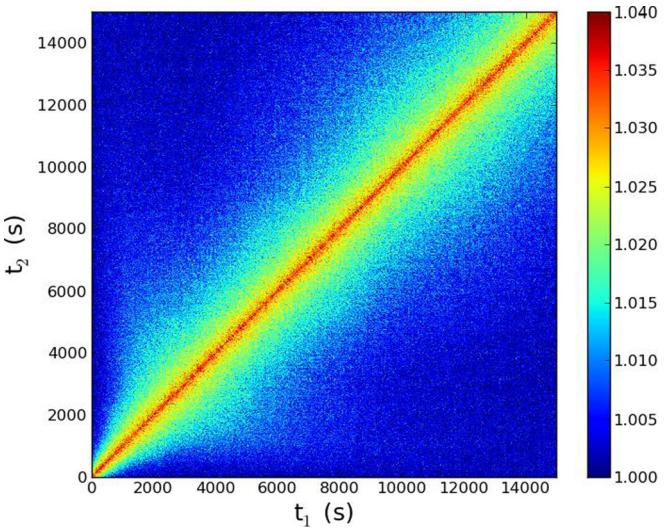

FIG. 2. TTCF measured with XPCS at 380 K after quenching from 385.5 K with 7 K min^{-1}. The broadening at short times due to equilibration stops after ∼2800 s.

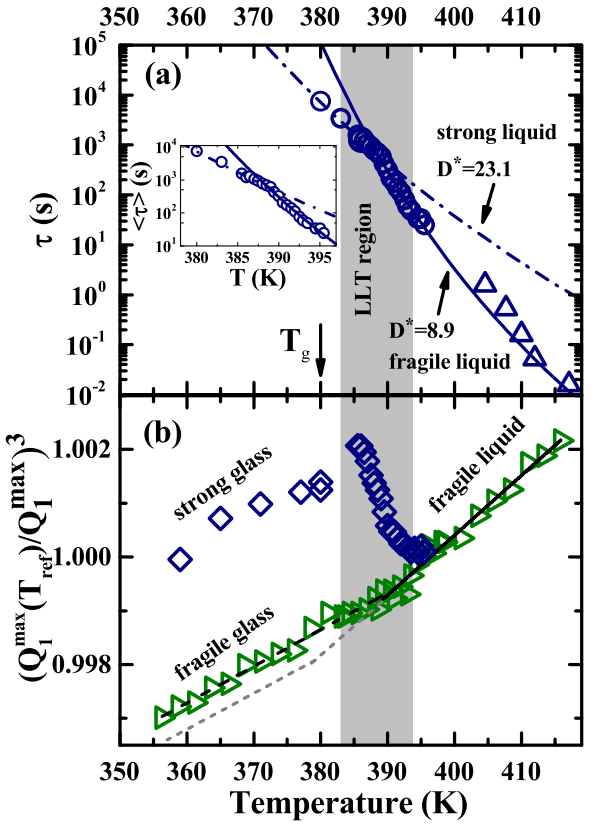

FIG. 3. (a) Temperature dependence of τ measured by XPCS (circles) and DMA (triangles). The LLT occurs at 389 K leading to two regimes with distinct fragilities (magnified in the inset). (b) Temperature dependence of the relative shift $[Q_1^{\max}(T_{\rm ref})/Q_1^{\max}]^3$ measured with XRD by continuous cooling with 1.5 K min^{-1} (green triangles), and by applying the quasistatic protocol used for XPCS (blue diamonds). The gray dashed line shows the standard behavior expected in the absence of the LLT.

than the corresponding relaxation time. This applies to all temperatures but 380 K (see Fig. 2). Here, we cooled the material from 385.5 K with a rate of 7 K min^{-1} to 380 K without any step. The system is not able to equilibrate during cooling and temporarily freezes into the glass from which it equilibrates in about 2800 s, as indicated by the continuous broadening of the intensity at the beginning of the measurement. After reaching equilibrium, the dynamics is stationary again and the system reaches the liquid, evidenced by a β of 0.71 ± 0.05. The corresponding $g_2(Q_p, t)$ is shown in Fig. 1(a). It should be noted that the equilibration of the ultraviscous liquid is highly promoted by down-jumps in temperature, while the equilibration from the as-quenched glass toward the liquid requires longer times than those probed here. As a consequence, the $g_2(Q_p, t)$ measured by heating the glass [Fig. 1(b)] remain compressed with fast relaxation times. Asymmetric equilibrations are typical of glass formers [43] and have been reported also in previous XPCS studies [30].

Figure 3(a) shows the temperature dependence of the mean relaxation time $\langle\tau\rangle = \Gamma(\frac{1}{\beta})\frac{\tau}{\beta}$ obtained from the XPCS data. A clear change in the trend is observed at 389 K where $\langle\tau\rangle$ evolves from a steep to a weaker temperature dependence. At first sight, one would intuitively associate this behavior with the glass transition. This interpretation is, however, *in contradiction* with several observations. (1) The change occurs at a temperature ≈10 K above the expected T_g. (2) The shape of the corresponding $g_2(Q_p, t)$ remains stretched without any signature of the stress-dominated dynamics of metallic glasses and reported in Fig. 1(b) for the studied alloy. (3) Evidence of an aging glass is observed only at the lowest investigated temperature of 380 K (Fig. 2), while at higher temperatures the TTCFs exhibit stationary dynamics [Fig. 1(c)].

B. Structural data

To better understand the dynamics, we employed XRD to investigate the structural changes occurring in the material while applying the *identical* thermal protocol. We find a transition from one liquid structure to a different one before the system freezes into a *glass*, which is different from that obtained by faster cooling. This reveals the existence of a complex dynamical pattern that cannot be associated to a simple glass transition.

XRD results are shown in Fig. 3(b) through the temperature dependence of the position of the first sharp diffraction peak (FSDP) of the static structure factor $[Q_p(T_{\rm ref})/Q_p(T)]^3$, with $T_{\rm ref} = 395.5$ K (see the Supplemental Material [20] for more details on the XRD data). During a standard vitrification, this quantity continuously decreases upon cooling and then bends over to a weaker temperature dependence at T_g, due to the kinetic arrest and the transition into one isoconfiguration of the glass. This is indeed the case for a second dataset (see the Supplemental Material [20] for more details on the XRD data), which has been taken by *continuously cooling* the liquid with a *faster rate* of 1.5 K min^{-1} (open triangles, $T_g = 390$ K).

By applying the quasistatic cooling, T_g is lowered to 380 K. Normally, one would simply expect to observe the same departure from the liquid at this lower temperature (dashed gray line in the figure). In stark contrast to this, $[Q_p(T_{\rm ref})/Q_p(T)]^3$ (blue diamonds) displays a steady anomalous increase between 395.5 and 385.5 K, thus above the expected T_g (see also the raw

XRD data in the Supplemental Material [20]). This increase indicates the occurrence of *pronounced structural changes* which *cannot* be associated to the vitrification. The bend of the data below 380 K also confirms a T_g of 380 K for the strong liquid. Additional data taken below this temperature decrease upon cooling with a slope similar to that of the fast-cooled glass (green open triangles). The observed structural changes imply the existence of *different liquid phases* and strongly resemble what has been reported during a LLT in a Zr-based liquid far above T_g [6].

III. DISCUSSION

In light of these observations, the dynamical crossover measured by XPCS [Fig. 3(a)] must be associated with the structural changes during the LLT. The data above and below 389 K can be fitted separately with a Vogel-Tammann-Fulcher (VFT) equation $\langle\tau\rangle = \tau_0 \exp(\frac{D^* T_0}{T - T_0})$, where τ_0 is the high-temperature relaxation time (10^{-14} s), D^* is the kinetic fragility, and T_0 is the temperature, at which τ would diverge within this empirical description. The high-temperature liquid exhibits a fragile behavior with $D^* = 8.9 \pm 0.4$ and $T_0 = 315.9 \pm 2.3$ K. This fit is in good agreement with the fragility obtained at higher temperatures from α-relaxation times [open triangles in Fig. 3(a)] measured using a dynamic mechanical analyzer (DMA) (see the Supplemental Material [20] for technical details on DMA). Differently, the low-temperature liquid is best fitted with $D^* = 23.1 \pm 0.8$ and $T_0 = 243.3 \pm 3$ K, showing a clearly stronger kinetic nature and, hence, a fragile-to-strong LLT in the ultraviscous state. Similar results can be obtained also with an Arrhenius model (see the comparison between VFT and the Arrhenius model reported in the Supplemental Material [20]). The value of D^* for the strong liquid is comparable to that of other strong metallic glass formers [44,45] close to T_g, whereas that for the fragile liquid is among the smallest reported in the literature [45,46]. In Zr-based glass formers, for example, such a fragile behavior is typically detected in the stable liquid well above the LLT [4,6,7].

Interestingly, the structure of the fragile high-temperature liquid evolves steadily towards the strong low-temperature liquid within a narrow temperature interval of 10 K, whereas the dynamical crossover occurs at a more defined temperature. Calorimetric studies show that the associated entropy change during the LLT is very small, i.e., 0.2 J g atom^{-1} K^{-1}, which is only 2.4% of the corresponding entropy of fusion [47]. This suggests the occurrence of extremely slow ordering kinetics during the LLT, as in other systems [25], which cannot be directly associated to a two-state crossover scenario [48].

As discussed before, the polyamorphic transition is not observed when the system is cooled with a faster rate. Here, T_g is close to the temperature of the dynamical transition [triangles in Fig. 3(b)], and the fragile liquid freezes into the glass before the LLT can occur. Between the two competing processes, vitrification is the dominant one. This is obvious if we consider that the glass transition is manifested by marked changes to dynamical quantities, while the structure of a glass is virtually indistinguishable from that of the corresponding supercooled liquid (isoconfigurational) at the moment of freezing. Without major structural modifications, vitrification occurs on a faster time scale than the order-driven LLT, which instead consists of time-consuming structural rearrangements in the highly viscous supercooled liquid probed here.

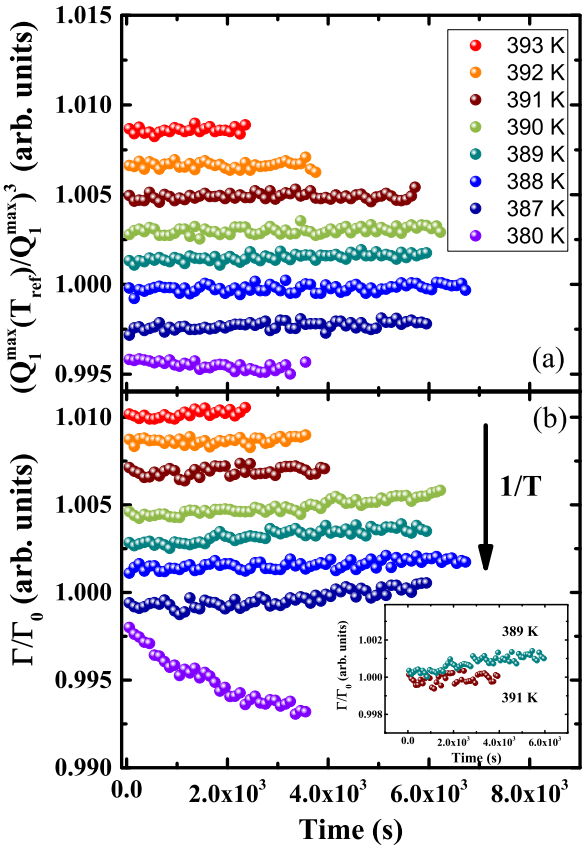

FIG. 4. Temporal evolution of $[Q_1^{\max}(T_{\rm ref})/Q_1^{\max}]^3$ (a) and FWHM (b) during isotherms at selected temperatures between 395.5 and 380 K. All data are vertically shifted. We distinguish three behaviors: (1) Between 395.5 K and 391 K, both $[Q_1^{\max}(T_{\rm ref})/Q_1^{\max}]^3$ and the FWHM are constant with time; (2) between 390 and 385.5 K $[Q_1^{\max}(T_{\rm ref})/Q_1^{\max}]^3$ remains constant while the FWHM slightly increases with time signaling changes in the local order; (3) at T_g (380 K) both parameters decrease due to the equilibration at short times from the glass toward the liquid.

It is important to stress that the XRD data do not allow speculation on the evolution of the density during the LLT, as the correlation between the macroscopic density and $1/Q^3$ is not straightforward for multicomponent liquids [13]. In Zr-based metallic glass formers, for instance, the LLT is accompanied by tiny structural changes (as those reported here) but without any anomaly in the density [6,7]. There, the LLT is driven more by changes in the entropy and in the local (chemical) order than by density changes. This could be the case also in our system.

We can get some indication on the density from the XPCS data as a change in density would reflect in a change in the decay of the density fluctuations and thus in the $g_2(Q_p, t)$. The XPCS data show that the density changes only with temperature, although without further information, while it remains constant during the isotherms. This is in agreement with the constant value of $[Q_p(T_{\rm ref})/Q_p(T)]^3$ during the isotherms (See Fig. 4(a) and the Supplemental Material [20]

for more details on the XRD data) and with a dynamic-to-structure connection recently proposed [49]. In contrast, the relative change of the full width at half maximum (FWHM), $\Gamma/\Gamma_0(T_{\rm ref})$, of the FSDP exhibits a small, but still significant increase with time in the transition region below 391 K, whereas there is no evidence of changes above (Fig. 4(b), inset and XRD data in the Supplemental Material [20]). This behavior, together with the stationary dynamics observed with XPCS, suggests the existence of local rearrangements which do not affect the average density. At 380 K, instead, both parameters in Fig. 4 decrease with time as a consequence of the aging towards the equilibrium [49] (see also the raw XRD data in the Supplemental Material [20]). As shown in Fig. 2, at this low temperature, the system freezes into the glass upon cooling and subsequently equilibrates within ∼2800 s. This can be attributed to a densification and ordering process during aging [38,49].

IV. CONCLUSIONS

In conclusion, we report microscopic evidence of the direct connection at the atomic level between polyamorphism and fragile-to-strong dynamical crossover in an ultraviscous metallic glass former. In the specific system studied in this work, this phenomenology is usually hidden by the vitrification at higher cooling rates and appears associated with the slow formation of a distinct local order without affecting the average density [21,24]. This scenario shares similarities with the LLTs reported at high temperatures in Zr-based alloys [6,7], and with the case of supercooled triphenyl phosphite [16,17,25], where the transitions are also accompanied by structural changes not affecting the density, without a direct microscopic connection to a fragile-to-strong dynamical crossover.

Finally, it is worth briefly discussing our results in light of the current discussions about a possible divergence [50] or not [51–53] of the dynamics below the conventional T_g. Our findings show a specific case where a sudden change in the temperature dependence of the relaxation time in the ultraviscous regime comes from subtle structural changes in the liquid and not from a dynamical divergence, which could, however, still occur at lower temperatures.

ACKNOWLEDGMENTS

We gratefully thank the ESRF and DESY for providing beamtime. H. Vitoux, K. L'Hoste, and F. Zontone are acknowledged for their support during the XPCS measurements at ESRF, Y. Chushkin for providing the code for the analysis of the XPCS data, J. Bednarcik for the support during the XRD measurements at DESY, and J. Wright for the support at ESRF. We gratefully thank H. Tanaka for discussions and a careful reading of the manuscript. W. Hembree and V. M. Giordano are also thanked for useful discussions. I.G. acknowledges financial support from the DFG Grant No. GA 1721/2-2. E.P. acknowledges financial support from MINECO, Grant No. FIS2014-54734-P, and Generalitat de Catalunya, Grant No. 2014SGR00581.

[1] P. F. McMillan, M. Wilson, D. Daisenberger, and D. Machon, Nat. Mater. **4**, 680 (2005).
[2] S. Sastry and C. Austen Angell, Nat. Mater. **2**, 739 (2003).
[3] M. H. Bhat, V. Molinero, E. Soignard, V. C. Solomon, S. Sastry, J. L. Yarger, and C. A. Angell, Nature **448**, 787 (2007).
[4] C. Way, P. Wadhwa, and R. Busch, Acta Mater. **55**, 2977 (2007).
[5] Z. Evenson, T. Schmitt, M. Nicola, I. Gallino, and R. Busch, Acta Mater. **60**, 4712 (2012).
[6] S. Wei, F. Yang, J. Bednarcik, I. Kaban, O. Shuleshova, A. Meyer, and R. Busch, Nat. Commun. **4**, 2083 (2013).
[7] M. Stolpe, I. Jonas, S. Wei, Z. Evenson, W. Hembree, F. Yang, A. Meyer, and R. Busch, Phys. Rev. B **93**, 014201 (2016).
[8] S. Aasland and P. F. McMillan, Nature **369**, 633 (1994).
[9] Y. Katayama, T. Mizutani, W. Utsumi, O. Shimomura, M. Yamakata, and K. Funakoshi, Nature **403**, 170 (2000).
[10] I. Saika-Voivod, P. H. Poole, and F. Sciortino, Nature **412**, 514 (2001).
[11] V. Molinero, S. Sastry, and C. A. Angell, Phys. Rev. Lett. **97**, 075701 (2006).
[12] A. Jaiswal, A. Podlesynak, G. Ehlers, R. Mills, S. O'Keeffe, J. Stevick, J. Kempton, G. Jelbert, W. Dmowski, K. Lokshin, T. Egami, and Y. Zhang, Phys. Rev. B **92**, 024202 (2015).
[13] W. Xu, M. T. Sandor, Y. Yu, H.-B. Ke, H.-P. Zhang, M.-Z. Li, W. H. Wang, L. Liu, and Y. Wu, Nat. Commun. **6**, 7696 (2015).
[14] P. Gallo, K. Amann-Winkel, C. A. Angell, M. A. Anisimov, F. Caupin, C. Chakravarty, E. Lascaris, T. Loerting, A. Z. Panagiotopoulos, J. Russo, J. A. Sellberg, H. E. Stanley, H. Tanaka, C. Vega, L. Xu, and L. G. M. Pettersson, Chem. Rev. **116**, 7463 (2016).
[15] S. Wei, M. Stolpe, O. Gross, W. Hembree, S. Hechler, J. Bednarcik, R. Busch, and P. Lucas, Acta Mater. **129**, 259 (2017).
[16] R. Kurita and H. Tanaka, Phys. Rev. Lett. **95**, 065701 (2005).
[17] R. Kurita, Y. Shinohara, Y. Amemiya, and H. Tanaka, J. Phys.: Condens. Matter **19**, 152101 (2007).
[18] C. A. Angell, MRS Bull. **33**, 544 (2011).
[19] A. Faraone, L. Liu, C.-Y. Mou, C.-W. Yen, and S. H. Chen, J. Chem. Phys. **121**, 10843 (2004).
[20] See Supplemental Material at http://link.aps.org/supplemental/10.1103/PhysRevMaterials.2.085603 for more information on the experimental methods and the raw XPCS and XRD data.
[21] H. Tanaka, Phys. Rev. E **62**, 6968 (2000).
[22] H. Tanaka, R. Kurita, and H. Mataki, Phys. Rev. Lett. **92**, 025701 (2004).
[23] K. Murata and H. Tanaka, Nat. Mater. **11**, 436 (2012).
[24] H. Tanaka, Eur. Phys. J. E **35**, 113 (2012).
[25] M. Kobayashi and H. Tanaka, Nat. Commun. **7**, 13438 (2016).
[26] Z. Evenson, S. E. Naleway, S. Wei, O. Gross, J. J. Kruzic, I. Gallino, W. Possart, M. Stommel, and R. Busch, Phys. Rev. B **89**, 174204 (2014).
[27] B. Ruta, G. Monaco, V. M. Giordano, F. Scarponi, D. Fioretto, G. Ruocco, K. S. Andrikopoulos, and S. N. Yannopoulos, J. Phys. Chem. B **115**, 14052 (2011).
[28] A. Madsen, A. Fluerasu, and B. Ruta, in *Synchrotron Light Sources and Free-Electron Lasers* (Springer International Publishing, Cham, 2015), pp. 1–21.

[29] L. Cipelletti, L. Ramos, S. Manley, E. Pitard, D. A. Weitz, E. E. Pashkovski, and M. Johansson, Faraday Discuss. **123**, 237 (2003).
[30] B. Ruta, Y. Chushkin, G. Monaco, L. Cipelletti, E. Pineda, P. Bruna, V. M. Giordano, and M. Gonzalez-Silveira, Phys. Rev. Lett. **109**, 165701 (2012).
[31] L. Berthier, Physics **4**, 42 (2011).
[32] D. Richter, B. Frick, and B. Farago, Phys. Rev. Lett. **61**, 2465 (1988).
[33] P. Lunkenheimer, R. Wehn, U. Schneider, and A. Loidl, Phys. Rev. Lett. **95**, 055702 (2005).
[34] N. B. Olsen, T. Christensen, and J. C. Dyre, Phys. Rev. Lett. **86**, 1271 (2001).
[35] Z. Evenson, B. Ruta, S. Hechler, M. Stolpe, E. Pineda, I. Gallino, and R. Busch, Phys. Rev. Lett. **115**, 175701 (2015).
[36] B. Ruta, V. M. Giordano, L. Erra, C. Liu, and E. Pineda, J. Alloys Compd. **615**, 45 (2014).
[37] B. Ruta, G. Baldi, G. Monaco, and Y. Chushkin, J. Chem. Phys. **138**, 54508 (2013).
[38] B. Ruta, E. Pineda, and Z. Evenson, J. Phys.: Condens. Matter **29**, 503002 (2017).
[39] P. Chaudhuri and L. Berthier, Phys. Rev. E **95**, 060601(R) (2017).
[40] E. E. Ferrero, K. Martens, and J. L. Barrat, Phys. Rev. Lett. **113**, 248301 (2014).
[41] M. Bouzid, J. Colombo, L. V. Barbosa, and E. Del Gado, Nat. Commun. **8**, 15846 (2016).
[42] B. Ruta, Y. Chushkin, G. Monaco, L. Cipelletti, V. M. Giordano, E. Pinead, and P. Bruna, in *Proceedings of 4th international Symposium on Slow Dynamics in Complex Systems, Sendai, Japan, 2012*, edited by M. Tokuyama and I. Oppenheim, AIP Conf. Proc. No. 1518 (AIP, New York, 2013), p. 181.
[43] C. A. Angell, K. L. Ngai, G. B. McKenna, P. F. McMillan, and S. W. Martin, J. Appl. Phys. **88**, 3113 (2000).
[44] R. Busch, W. Liu, and W. L. Johnson, J. Appl. Phys. **83**, 4134 (1998).
[45] I. Gallino, J. Schroers, and R. Busch, J. Appl. Phys. **108**, 063501 (2010).
[46] O. Gross, B. Bochtler, M. Stolpe, S. Hechler, W. Hembree, R. Busch, and I. Gallino, Acta Mater. **132**, 118 (2017).
[47] I. Gallino, D. Cangialosi, Z. Evenson, L. Schmitt, S. Hechler, M. Stolpe, and B. Ruta, Acta Mater. **144**, 400 (2018).
[48] H. Tanaka, J. Phys.: Condens. Matter **15**, L703 (2003).
[49] V. M. Giordano and B. Ruta, Nat. Commun. **7**, 10344 (2015).
[50] G. Adam and J. H. Gibbs, J. Chem. Phys. **43**, 139 (1965).
[51] J. Zhao, S. L. Simon, and G. B. Mckenna, Nat. Commun. **4**, 1783 (2013).
[52] E. Arianna, A. Pogna, C. Rodríguez-Tinoco, G. Cerullo, C. Ferrante, and J. Rodríguez-viejo, Proc. Natl. Acad. Sci. USA **112**, 2331 (2015).
[53] T. Hecksher, A. I. Nielsen, N. B. Olsen, and J. C. Dyre, Nat. Phys. **4**, 737 (2008).